Elastic Constants, Bulk Modulus, and Compressibility of H_2O Ice I*h* for the Temperature Range 50 K–273 K

Cite as: J. Phys. Chem. Ref. Data **47**, 033101 (2018); https://doi.org/10.1063/1.5030640
Submitted: 23 March 2018 . Accepted: 04 June 2018 . Published Online: 05 July 2018

J. J. Neumeier

Elastic Constants, Bulk Modulus, and Compressibility of H_2O Ice I*h* for the Temperature Range 50 K–273 K

J. J. Neumeier[a)]

Physics Department, Montana State University, Bozeman, Montana 59717-3840, USA

(Received 23 March 2018; accepted 4 June 2018; published online 5 July 2018)

Published elastic constant data for H_2O ice in the I*h* phase are compiled and evaluated. Fits of the five elastic constants for $50 \leq T/\mathrm{K} \leq 273$ are conducted to yield a reliable and convenient source for elastic constant values. Various elastic properties can be calculated from the elastic constants obtained herein. The elastic constants are used to determine the adiabatic bulk modulus B_S for the same temperature range with an estimated uncertainty of less than 1.3%. Fitting those data yields an equation for B_S that is extrapolated to provide values for $0 \leq T/\mathrm{K} < 50$. The adiabatic compressibility K_S, isothermal bulk modulus B_T, and isothermal compressibility K_T are calculated from B_S. Comparisons are made to published data. *Published by AIP Publishing on behalf of the National Institute of Standards and Technology.* https://doi.org/10.1063/1.5030640

Key words: bulk modulus; compressibility; elastic constants, H_2O ice; thermodynamic properties.

CONTENTS

1. Introduction 1
2. The Elastic Constant Data 2
3. Determination of the Bulk Modulus and Compressibility 3
4. Conclusions 6
Acknowledgments 6
5. Appendix A: Measurement Uncertainties 6
6. Appendix B: Equations 7
7. Appendix C: Deviation of Fits from the Measurement Data 7
8. References 7

List of Tables

1. Elastic constants c_{ij}, adiabatic bulk modulus B_S, adiabatic compressibility K_S, isothermal bulk modulus B_T, isothermal compressibility K_T, and $TV\beta^2/C_P$ for ice I*h*[a] 4

List of Figures

1. Elastic constants c_{11} (a) and c_{33} (b) versus temperature for ice I*h* 2
2. Elastic constants c_{44} (a) and c_{12} (b) versus temperature for ice I*h* 3
3. Elastic constants c_{13} versus temperature for ice I*h* 3
4. Adiabatic bulk modulus B_S versus temperature T for ice I*h* 5
5. Isothermal compressibility K_T versus temperature T for ice I*h* 5
6. Deviations of the measured elastic constants c_{11}, c_{33}, and c_{12} from their polynomial fits versus temperature 6

1. Introduction

Solid H_2O at ambient pressure exists in a hexagonal crystal structure[1] known as ice I*h*. Few direct measurements of its isothermal compressibility $K_T = -(1/V)(\mathrm{d}V/\mathrm{d}P)_T$, where V is the volume, P is the hydrostatically applied pressure, and T is the temperature, have been published. A value of 3.6×10^{-10} Pa^{-1} reported in 1912 seems to be erroneous[2] when compared to a measurement in 1914 by Richards and Speyers[3] of $K_T = 1.20(1) \times 10^{-10}$ Pa^{-1} at 266.1 K and two more recent measurements, $1.10(12) \times 10^{-10}$ Pa^{-1} determined from the linear compressibilities[4] at 263 K and $1.015(46) \times 10^{-10}$ Pa^{-1} obtained[5] from neutron diffraction at 145 K. The compressibility can be determined from elastic constants, and numerous measurements of the five elastic constants c_{ij} have been made. The elastic constants are acquired from sound velocity or other rapid measurement techniques[6] where no heat enters the sample during the time scale of the measurement. As a result, the compressibility obtained from them[6] is at constant entropy S. For most solids, the isoentropic, or adiabatic, compressibility, K_S, differs only slightly from K_T, and the difference

[a)]neumeier@montana.edu

Published by AIP Publishing on behalf of the National Institute of Standards and Technology.

is easily calculated from K_S using the temperature, heat capacity, volume, and thermal expansion coefficient. In the case of ice, the difference can be as large as 3% near 273 K since its thermal expansion coefficient is a few times larger than that of common solids.

Values of K_T and K_S (or the bulk moduli $B_T = 1/K_T$ and $B_S = 1/K_S$) calculated from elastic constants appear in some compilations. In one case, K_S was calculated at seven temperatures[7] using the available c_{ij} values, with assumptions made regarding some unavailable values. An equation of state[8,9] for ice I*h*, which utilized the elastic constant data and a host of other data for its creation, has been used to calculate K_T and K_S for $0 \leq T/\mathrm{K} \leq 273$. The present work aims to compile and fit the existing c_{ij} data in order to provide a complete set of c_{ij} values for the broadest possible temperature range with the goal of determining B_S, B_T, K_S, and K_T. The resulting c_{ij}'s are useful for the calculation of other elastic properties, such as shear moduli and anisotropy constants.[10] The c_{ij}'s are used to calculate B_S for the temperature range $50 \leq T/\mathrm{K} \leq 273$. An extrapolation based on the Wachtman equation[11] is conducted to provide estimated values for B_S down to $T = 0$ K. The analysis leads to a reliable, well-documented, and easy-to-use set of values for c_{ij} for the range $50 \leq T/\mathrm{K} \leq 273$ and B_S, B_T, K_S, and K_T for the range $0 \leq T/\mathrm{K} \leq 273$.

2. The Elastic Constant Data

Jona and Scherrer measured all c_{ij} values at 257 K through the observation of diffraction patterns of vibrating single crystals.[12] Bass *et al.*[13] measured the resonance frequencies of plates and rods of oriented single-crystalline ice in the frequency range 5–50 kHz between 243 K and 273 K to determine the elastic constants. Zarembovitch and Kahane measured the sound velocity and obtained c_{11} and c_{33} over the temperature range $93 < T/\mathrm{K} < 271$.[14] Bogorodskii determined all c_{ij} values from sound-velocity measurements at 258, 263, and 273 K.[15] Proctor measured the sound velocity and determined c_{11} and c_{33} for $50 < T/\mathrm{K} < 250$ and c_{44}, c_{12}, and c_{13} for $60 < T/\mathrm{K} < 110$.[16] Dantl measured the sound velocity and determined all c_{ij} values for the temperature range $133 < T/\mathrm{K} < 273$.[17,18] In more recent years, Brillouin spectroscopy was used to determine all c_{ij}'s at 238 K, 257 K, and 270 K.[19–21] The measurement uncertainties of c_{ij} and T associated with each of these studies are provided in Appendix A.

The agreement of specific c_{ij} values obtained by the researchers is not ideal. The discrepancies among the data sets and lack of available data over the entire temperature range of interest ($0 \leq T/\mathrm{K} \leq 273$) required that the data for each c_{ij} be assessed with the goal of obtaining the largest possible fitting region. Each c_{ij} data set was plotted and considered for inclusion in the fitting process. The details of this process are clarified below. No conversions of the published temperature values to a modern temperature scale, such as the International Temperature Scale of 1990 (ITS-90), were made, since each of the studies made little mention of how the temperature and the associated uncertainties were determined (see Appendix A).

The data for c_{11} are shown in Fig. 1(a). The data agree extremely well with one another, with the exception of the data of Dantl and of Bogorodskii. The data of Dantl for both c_{11} and c_{33} [see Fig. 1(b)] appear to be plagued with a systematic error; they lie about 7% below those of five other reports. For this reason, these data were excluded from the fitting. The data point of Bass *et al.*[13] at 257.15 K (not included in the plot) falls on top of the Dantl data and was not included in the fitting. Substantial scattering of the data from Bogorodskii exists for most c_{ij} values; they were excluded from the fitting of c_{11}. For fitting the data, a second-order polynomial was used. The fit is shown along with the data in Fig. 1(a). The situation for c_{33} is similar. The fitting excluded the data of Dantl, Bogorodski, and Bass *et al.* The resulting fit and the data are shown in Fig. 1(b). The fit parameters for c_{11} and c_{33} are provided in Appendix B and the deviations of the fits from the data used in the fitting are discussed in Appendix C. The deviations from the fit are below about 0.5% for the most part, except for a few extraneous points that range up to 1.3%.

The data for c_{44} are shown in Fig. 2(a). A substantial discontinuity is present between the data of Dantl and Proctor; each of these data sets covers a limited temperature range due to various experimental difficulties.[16,17] The data of Bogorodskii were excluded from the fitting. A simple second-order polynomial was unable to fit the data. Instead, we used a slight modification of the Wachtman equation,[11] which is sometimes used to fit elastic constants.[16] The Wachtman equation worked well in fitting the

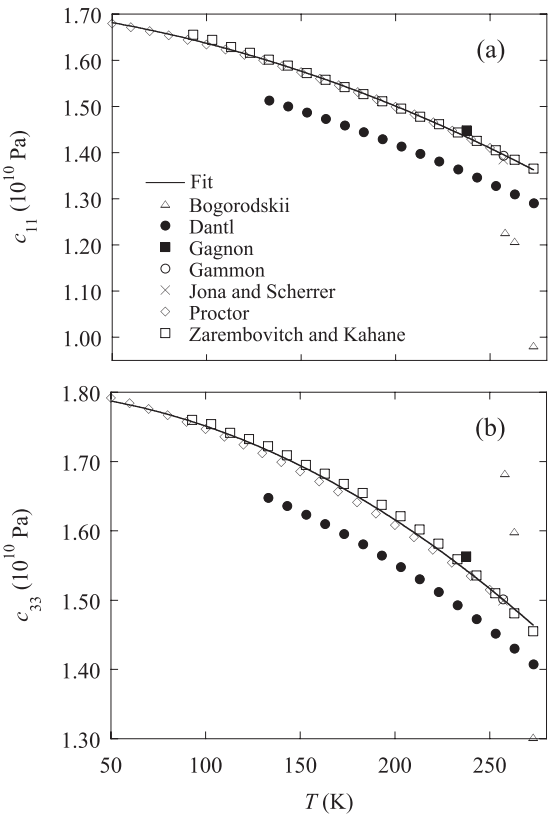

FIG. 1. Elastic constants c_{11} (a) and c_{33} (b) versus temperature for ice I*h*. The data points are from the published literature as indicated. The solid lines are fits to the data as described in the text. The fit parameters are provided in Appendix B.

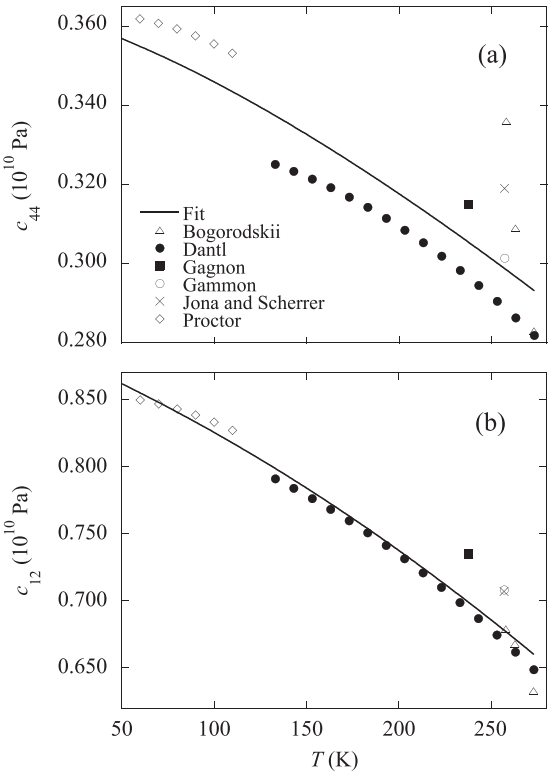

FIG. 2. Elastic constants c_{44} (a) and c_{12} (b) versus temperature for ice I*h*. The data points are from the published literature as indicated. The solid lines are fits to the data as described in the text. The fit parameters are provided in Appendix B.

Young's modulus Y of Al_2O_3. It is an empirical equation, whose thermodynamic basis has been explained.[11] On thermodynamic grounds, $\partial c_{ij}/\partial T \to 0$ as $T \to 0$ and $\partial c_{ij}/\partial T$ approaches a constant at very high temperatures.[16,22] The Wachtman equation, given by $Y = Y_0 - aT\mathrm{e}^{-T_0/T}$, satisfies these requirements. Attempts to fit c_{44} required a slight change to the exponent of T from 1 to 1.35; this exponent was needed to capture the curvature of the data. The resulting equation for c_{44} is provided in Appendix B. The data of Bogorodskii were excluded from this fit. Although the data extended only to 60 K, the fit, a well-behaved function, was extrapolated to obtain c_{44} values to 50 K.

The data for c_{12} are shown in Fig. 2(b). The data were fitted to a second-degree polynomial, which is shown as the solid line. In this case, all data were included in the fitting. Although the data extended only to 60 K, the fit, a well-behaved function, was extrapolated to obtain points to 50 K. The fit parameters for c_{12} are provided in Appendix B and the deviations of the fit from the data used in the fitting are discussed in Appendix C. The deviations are for the most part below about 1.6%, except for a few extraneous points that range up to 5%. The data for c_{13} are shown in Fig. 3. Note that the data of Dantl and of Proctor are essentially linear, but with different slopes. This along with the substantial discontinuity between the two data sets made fitting impossible. Instead of fitting, the equation[23]

$$c_{13} = c_{11} + c_{12} - c_{33} \tag{1}$$

was used to determine c_{13} through use of the fits described above for c_{11}, c_{33}, and c_{12}. The result is shown as the solid line

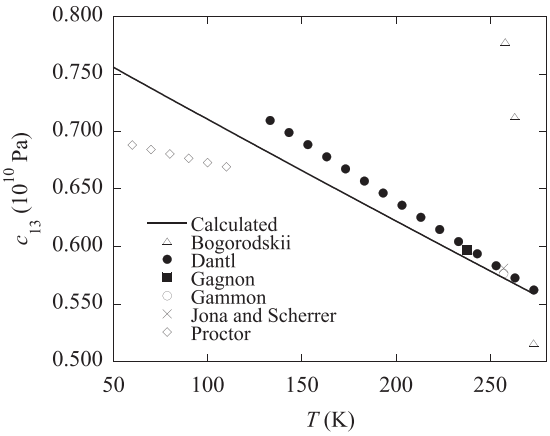

FIG. 3. Elastic constants c_{13} versus temperature for ice I*h*. The data points are from the published literature. The solid line is calculated from $c_{13} = c_{11} + c_{12} - c_{33}$, using the fits for c_{11}, c_{33}, and c_{12}.

in Fig. 3 and tabulated in Table 1. It is fairly linear and falls between the existing data sets, deviating from the experimental data of Proctor and of Dantl by less than 8%. Using Eq. (1) and the deviations of the polynomial fits of c_{11}, c_{33}, and c_{12} from the data, the uncertainty of c_{13} is estimated at 2.5% or less. The data from our calculation at 257.15 K is about 15% larger than the value given by Bass *et al.*,[13] but their value has uncertainty of nearly 20%, and it is significantly smaller than the value of Jona and Scherrer.[12] A fit to our result for c_{13} using a second-order polynomial was conducted, the parameters of which are provided in Appendix B for convenience.

A few aspects are discussed here. Note that c_{44} can be calculated[23] according to

$$c_{44} = \frac{(c_{33} - c_{13})^2}{2(c_{33} - 5c_{13} + 4c_{12})}. \tag{2}$$

This was carried out using the fits obtained above. The resulting c_{44} is about 8% larger in magnitude than the fit shown in Fig. 2(a). Since c_{44} is not needed for subsequent calculations herein, this observation is simply brought to the reader's attention. Using the data in Table 1 and Eq. (2), the reader can calculate c_{44} if desired. It is noteworthy that the c_{33} elastic constant of ice I*h* exhibits a dip of about 6% in magnitude in the temperature region of $80 < T/\mathrm{K} < 150$ if cooled at a rate above 0.7 K/min.[24] This feature did not appear in the purest ice samples and was sometimes studied in samples doped with HF (3×10^{-4} mol/l). The physical origin of the feature was attributed to proton disorder. This effect was neglected in the fitting presented herein but may be important for those studying this temperature region.[25]

3. Determination of the Bulk Modulus and Compressibility

When a hexagonal single crystal is subjected to uniform pressure, the volume compressibility K_S is easily obtained[26] using the compliance tensor, resulting in

TABLE 1. Elastic constants c_{ij}, adiabatic bulk modulus B_S, adiabatic compressibility K_S, isothermal bulk modulus B_T, isothermal compressibility K_T, and $TV\beta^2/C_P$ for ice Ih[a]

T (K)	c_{11} (10^{10} Pa)	c_{33} (10^{10} Pa)	c_{12} (10^{10} Pa)	c_{13} (10^{10} Pa)	c_{44} (10^{10} Pa)	B_S (10^{10} Pa)	K_S (10^{-10} Pa^{-1})	B_T (10^{10} Pa)	K_T (10^{-10} Pa^{-1})	$\frac{TV\beta^2}{C_P}$ (10^{-12} Pa^{-1})
0	...	...	...	...	...	1.133	0.8825	1.133	0.8825	0
10	...	...	...	...	...	1.126	0.8880	1.126	0.8880	0
20	...	...	...	...	...	1.119	0.8935	1.119	0.8936	0.011
30	...	...	...	...	...	1.112	0.8990	1.112	0.8992	0.021
40	...	...	...	...	...	1.105	0.9047	1.105	0.9049	0.018
50	1.682	1.787	0.8617	0.7559	0.3539	1.100	0.9093	1.100	0.9094	0.007
60	1.674	1.782	0.8548	0.7467	0.3529	1.092	0.9160	1.092	0.9160	0
70	1.665	1.776	0.8477	0.7377	0.3517	1.084	0.9228	1.084	0.9229	0.007
80	1.656	1.768	0.8405	0.7287	0.3503	1.075	0.9301	1.075	0.9304	0.033
90	1.647	1.760	0.8331	0.7197	0.3486	1.067	0.9376	1.066	0.9384	0.081
100	1.637	1.751	0.8254	0.7107	0.3466	1.058	0.9456	1.056	0.9471	0.149
110	1.626	1.742	0.8175	0.7017	0.3446	1.048	0.9539	1.046	0.9563	0.238
120	1.614	1.731	0.8095	0.6928	0.3420	1.039	0.9626	1.035	0.9660	0.340
130	1.602	1.720	0.8012	0.6839	0.3394	1.029	0.9717	1.024	0.9768	0.512
140	1.590	1.707	0.7927	0.6750	0.3366	1.019	0.9813	1.012	0.9880	0.670
150	1.576	1.694	0.7840	0.6661	0.3336	1.009	0.9913	1.000	0.9997	0.848
160	1.562	1.680	0.7752	0.6573	0.3305	0.9983	1.002	0.9879	1.012	1.056
170	1.548	1.666	0.7661	0.6485	0.3272	0.9875	1.013	0.9752	1.026	1.277
180	1.533	1.650	0.7568	0.6397	0.3238	0.9764	1.024	0.9622	1.039	1.510
190	1.517	1.633	0.7472	0.6309	0.3202	0.9650	1.036	0.9489	1.054	1.761
200	1.501	1.616	0.7375	0.6222	0.3164	0.9534	1.049	0.9353	1.069	2.039
210	1.484	1.598	0.7276	0.6134	0.3126	0.9416	1.062	0.9214	1.085	2.328
220	1.466	1.579	0.7175	0.6047	0.3086	0.9294	1.076	0.9073	1.102	2.621
230	1.448	1.559	0.7071	0.5960	0.3046	0.9170	1.091	0.8934	1.119	2.879
240	1.429	1.538	0.6966	0.5874	0.3004	0.9043	1.106	0.8796	1.137	3.109
250	1.410	1.517	0.6859	0.5787	0.2961	0.8914	1.122	0.8661	1.155	3.274
260	1.390	1.494	0.6749	0.5701	0.2917	0.8782	1.139	0.8529	1.173	3.338
270	1.369	1.471	0.6637	0.5615	0.2872	0.8647	1.157	0.8400	1.191	3.402
273	1.363	1.464	0.6604	0.5589	0.2858	0.8606	1.162	0.8361	1.196	3.402

[a]The uncertainties of the c_{ij} values are discussed in the text and in Appendix C. The uncertainties for B_S, K_S, B_T, and K_T are estimated to be ±1.3%, ±1.3%, ±1.5%, and ±1.5%, respectively.

$$K_S = 2(s_{11} + s_{12} + 2s_{13}) + s_{33}, \tag{3}$$

where the s_{ij}'s are the compliance tensor components. The elastic constants are related[26] to the s_{ij}'s by the following equations:

$$c_{11} + c_{12} = \frac{s_{33}}{s}, \tag{4a}$$

$$c_{11} - c_{12} = \frac{1}{s_{11} - s_{12}}, \tag{4b}$$

$$c_{13} = \frac{-s_{13}}{s}, \tag{4c}$$

$$c_{33} = \frac{s_{11} + s_{12}}{s}, \tag{4d}$$

and

$$c_{44} = \frac{1}{s_{44}}, \tag{4e}$$

where

$$s = s_{33}(s_{11} + s_{12}) - 2s_{13}^2. \tag{5}$$

Using Eqs. (3) and (4a)–(4e), the bulk modulus $B_S = 1/K_S$ is found to be[10,27]

$$B_S = \frac{2c_{11} + c_{33} + 2c_{12} + 4c_{13}}{9}. \tag{6}$$

This form of B_S is attributed to Reuss; its calculation requires the use of some approximations. The c_{ij} values obtained from the fits were used to determine B_S with Eq. (6), which is shown in Table 1 and Fig. 4. The uncertainty of B_S was estimated to be below 1.3% for the entire temperature range. This estimate is based on the deviations of the fits to the c_{ij} data from the measurement data (shown in Appendix C) when placed in Eq. (6).

The available c_{ij} data and the resulting values for B_S extend only to 50 K. It is possible, however, to estimate B_S for the region $0 \le T/\mathrm{K} < 50$. It is important to note that $K_T = K_S$ as $T \to 0$. This is evident upon inspection of Eq. (7), which is obtained by considering the change in volume of a system that is associated with independent changes in temperature and volume along with changes in pressure that are associated with independent changes in temperature and entropy. The result is given by

$$K_T - K_S = \frac{TV\beta^2}{C_P}, \tag{7}$$

where β is the volume thermal expansion coefficient and C_P is the isobaric heat capacity. Values for $TV\beta^2/C_P$ were

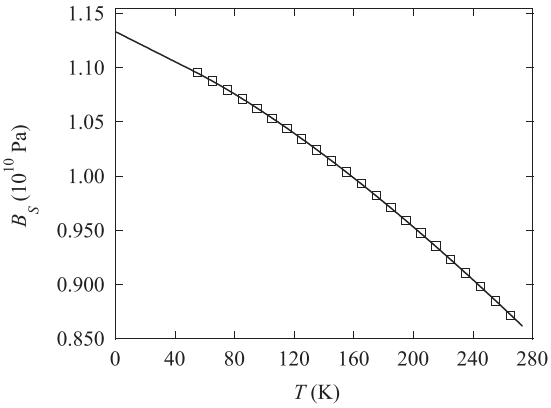

FIG. 4. Adiabatic bulk modulus B_S versus temperature T for ice I*h*. The data points were determined using the elastic constants. The solid line is a fit to the data for the range $50 \leq T/\mathrm{K} \leq 273$. It is extrapolated to $T = 0$.

determined using published volume,[1] volume thermal expansion coefficient,[28,29] and heat capacity[30,31] data and are provided in Table 1. The uncertainty is estimated at less than 1.4%, based on the uncertainties of each measured quantity[1,28,30] in Eq. (7). K_T is about 3% larger than K_S near 273 K, due to the relatively large magnitude of β for ice. The difference drops to 1.9% near 200 K and 0.16% at 100 K, and becomes still smaller at lower temperatures.

The Wachtman equation,[11] $Y = Y_0 - aTe^{-T_0/T}$, was used to fit the B_S data in order to extrapolate to $T = 0$ K. B_S is chosen for fitting since it is a better-behaved function than B_T due to the influence of Eq. (7) above 100 K. A variety of fits were attempted, including variations of the Wachtman equation and a simple second-order polynomial. Although a slightly better fit was obtained with the second-order polynomial, a good fit was obtained with $B_S = B_0 - aTe^{-T_0/T}$ with a slight change to the exponent of T from 1 to 1.35, which is needed to capture the curvature of B_S. The fit parameters B_0, a, and T_0 are provided in Appendix B. The difference between this fit and that using the polynomial was under 0.5% at $T = 0$. It is likely that the low melting point of ice compared to more common solids,[11] along with the complexities of proton disorder[25] and thermally stimulated molecular rotations[29,32] in ice, play roles in the difficulty of fitting B_S with the original form of the Wachtman equation. For example, the value of T_0 found for ice is about 1/30 of the value obtained[11] for Al_2O_3, and B_S of ice reveals substantial curvature in the range $50 < T/\mathrm{K} < 273$. More research would be needed to better understand these aspects. Figure 4 shows B_S obtained using the elastic constants for the region above 50 K as the data points along with the fit plotted to $T = 0$ K.

The temperature dependence of B_S below 50 K is comparable to that of other hexagonal solids.[10] Note that our values of B_S differ somewhat from the typically accepted values.[7,9,33] Comparing first to the data of Leadbetter,[7] they are approximately 16% (at 20 K) to 10% (at 260 K) smaller. This discrepancy is attributed to the fact that Leadbetter[7] used only the measured[14] elastic constants c_{11} and c_{33} to determine $K_S = 1/B_S$ and assumed that all other c_{ij}'s have the same temperature dependence. K_S has been calculated from the equation of state determined[9] for ice I*h*. The resulting data for $K_S = 1/B_S$ agree with those data within ~7% near 0 K, 4% near 50 K, 2% near 100 K, and 1% near 273 K. Table 1 provides a convenient reference for the values of B_S and K_S obtained through the procedure described above.

Equation (7) was used to determine K_T for the temperature range $0 \leq T/\mathrm{K} \leq 273$. Values are provided in Table 1, and the entire temperature range is plotted in Fig. 5 as the solid line. The uncertainty of K_T is 1.5%. The measured[3–5] values of K_T are provided in the figure along with their uncertainties. Data calculated from the equation of state[9] are also plotted, along with their reported uncertainty of about 1% (indicated on two data points). Notable is that K_T has only been measured *directly* four times, each time at a single temperature. The data point from Bridgman is excluded from the plot, since it is offscale.[2] The uncertainties in the measured data are sometimes large, which underscores the need for improved measurements of K_T. At 0 K, K_T determined from the equation of state is 6.8% *larger* than the value determined herein; at 273 K, it is 1.5% *smaller*; the agreement is quite good above 100 K. The discrepancy is associated with the fact that the measurements of each individual elastic constant from multiple reports were carefully considered in the present work to obtain B_S and K_S for the region above 50 K, which then lead to B_T and K_T. The resulting bulk moduli and compressibilities should be considered as measured values, with their associated uncertainties, since they were determined from the measured elastic constants and elastic theory. This level of analysis to obtain the bulk moduli and compressibilities was not conducted in Ref. 9, which had a much broader focus, involving multiple properties of H_2O ice. Furthermore, there is a significant discrepancy between the volume thermal expansion coefficient β, and its temperature dependence, below 75 K from recent high-resolution measurements[28,29] and the values calculated in Refs. 8 and 9. In their calculation, K_T and β are proportional to one another;[9] thus, their K_T needs updating to yield the correct temperature dependence below 75 K. Finally, the author stresses that the moduli values below 50 K presented

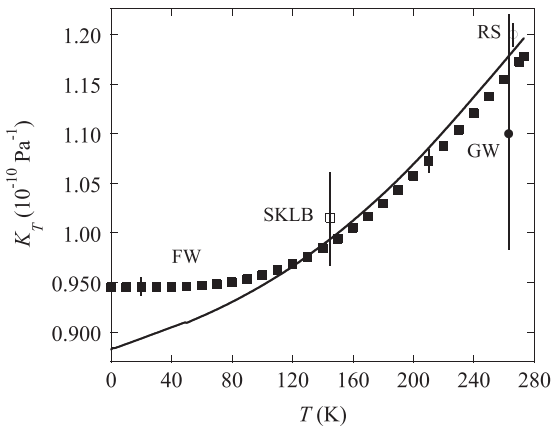

FIG. 5. Isothermal compressibility K_T versus temperature T for ice I*h*. The solid line is from the present work. The data points labeled FW are from the equation of state by Feistel and Wagner, SKLB from the work of Strassle *et al.*, GW from the work of Gow and Williamson, and RS from the work of Richards and Speyers. The vertical lines indicate the error reported for each datum or data set.

herein are based purely on an extrapolation and should be used with appropriate caution until data from direct measurements of the elastic constants or K_T become available.

4. Conclusions

Published elastic constant data were compiled and fitted to provide the five c_{ij} values for ice I*h* for the temperature range $50 \leq T/\mathrm{K} \leq 273$. The c_{ij}'s may prove useful for the calculation of elastic properties, such as shear moduli and anisotropy constants. Such calculations are well described in the literature.[10] The elastic constants were used to determine the bulk modulus of ice at constant entropy for $50 \leq T/\mathrm{K} \leq 273$, and an extrapolation based on empirical observations and the third law of thermodynamics[11] was used to find values to absolute zero temperature. The results were then used to find K_S, K_T, and B_T. The obtained K_T values were compared to the values from direct measurements, of which there exist few, and also compared to values determined through an equation of state. The agreement is very good above 100 K. The bulk moduli and compressibility values obtained herein, while not determined from direct compressibility measurements, are determined from elastic constant measurements, elastic theory, and a fundamental thermodynamic relation. They should be the most reliable values that are presently available. Given the complexity of ice I*h*, it is conceivable that some features exist in the bulk moduli and compressibility that the present analysis would never reveal. This is the case for the thermal expansion coefficient of ice, where recent measurements[29] revealed a large feature at 101 K, and the c_{33} elastic constant of ice I*h* which was shown[24] to exhibit a dip of about 6% in magnitude in the temperature region of $80 < T/\mathrm{K} < 150$. Ideally, direct, high-precision measurements of K_T should be conducted over the entire temperature range, especially for the region below 50 K. Until such data are available, the values provided herein should serve most purposes.

Acknowledgments

This work was supported by the National Science Foundation under Contract No. DMR-1204146.

5. Appendix A: Measurement Uncertainties

The measurement uncertainty reported in each elastic-constant publication is stated in this section. In all but three cases, no mention of the uncertainty in measuring T was provided. Bass *et al.*[13] reported uncertainties of 6%, 5%, 0.4%, 13%, and 20% for c_{11}, c_{33}, c_{44}, c_{12}, and c_{13}, respectively, at 257.15 K. Bogorodoskii states[15] only that the c_{ij} values possess uncertainties ranging up to 10%. The measured elastic constants from Dantl were fitted in that work to polynomials.[17] The stated deviations of the data from those fits were 0.3%, 0.4%, 0.7%, 2%, and 7% for c_{11}, c_{33}, c_{44}, c_{12}, and c_{13}, respectively. No mention was made regarding the absolute precision of the c_{ij} values,[17,18] although frequency sweeps at 263.15 K reveal scatter in the data below 1.5% for c_{11} and c_{33} and up to 2% for c_{44}. Gagnon *et al.*[21] reported uncertainty in T of ± 0.5 K and uncertainty of the elastic constants of less than 1%. The data of Gammon *et al.*[19,20] had stated uncertainties of 0.4%, 0.4%, 0.5%, 0.7%, and 0.6% for c_{11}, c_{33}, c_{44}, c_{12}, and c_{13}, respectively. In this case, the authors discussed their error sources in detail. No uncertainty in the measurement temperature of 270.15 K was provided in one instance,[19] but in their later measurements[20] at 257.15 K, the uncertainty in temperature was given as ± 0.5 K. A study by Green and Mackinnon[34] reported uncertainties of 3.8% and 2.5% for c_{33} and c_{44}, respectively, but failed to state the temperature at which the measurements were made. Jona and Scherrer measured the elastic constants at 257.15 K with uncertainties of 0.6%, 0.5%, 1%, 1.7%, and 2.7% for c_{11}, c_{33}, c_{44}, c_{12}, and c_{13}, respectively. Proctor[16] mentions that the temperature was determined via a thermocouple, with an uncertainty of ± 1 K. The c_{ij} values in that work were fitted to polynomials or the Wachtman equation; standard deviations of the coefficients were provided. The deviations of the data from the fits were found to be 0.2%, 0.3%, 1%, 1.2%, and 2% for c_{11}, c_{33}, c_{44},

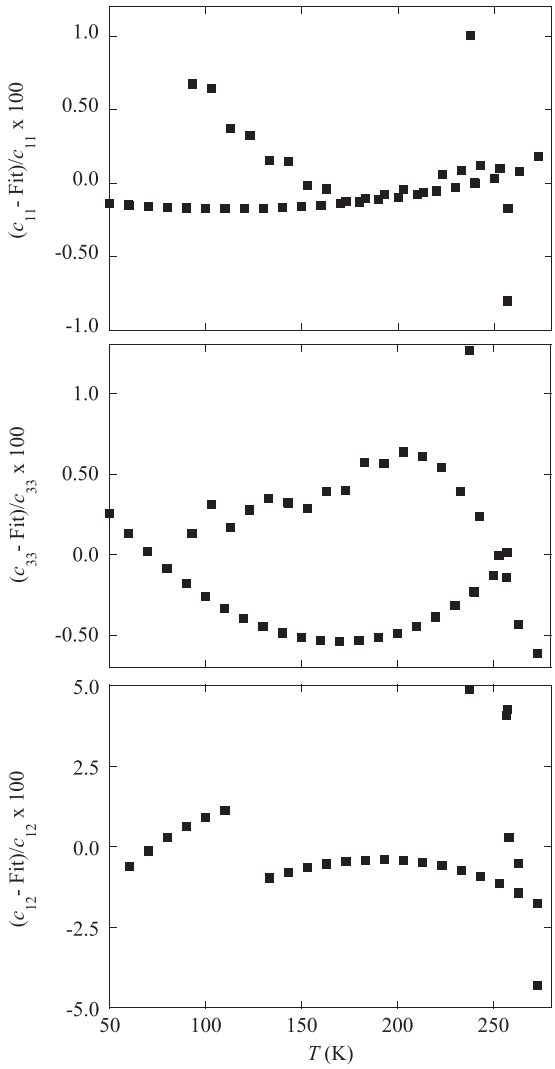

FIG. 6. Deviations of the measured elastic constants c_{11}, c_{33}, and c_{12} from their polynomial fits versus temperature.

c_{12}, and c_{13}, respectively. Zarembovitch and Kahane[14] measured c_{11} and c_{33} with uncertainties of 0.6% and 0.7%, respectively. The reported uncertainties for the elastic constants c_{12} and c_{13} are higher than the others, since their determination requires the use[12,16] of the measured values for c_{11}, c_{33}, and c_{44}.

6. Appendix B: Equations

The c_{ij} versus T data were fitted in the range $50 \leq T/\mathrm{K} \leq 273$ as clarified in the main text. The obtained fits are provided as follows:

$$c_{11} = (1.7111 \times 10^{10}\,\mathrm{Pa}) - (4.372 \times 10^{6}\,\mathrm{Pa/K})T - (30757\,\mathrm{Pa/K^2})T^2, \quad \text{(B1)}$$

$$c_{33} = (1.8023 \times 10^{10}\,\mathrm{Pa}) - (8.747 \times 10^{5}\,\mathrm{Pa/K})T - (42191\,\mathrm{Pa/K^2})T^2, \quad \text{(B2)}$$

$$c_{12} = (8.9266 \times 10^{9}\,\mathrm{Pa}) - (5.6951 \times 10^{6}\,\mathrm{Pa/K})T - (10308\,\mathrm{Pa/K^2})T^2, \quad \text{(B3)}$$

$$c_{44} = (3.5457 \times 10^{9}\,\mathrm{Pa}) - (5.629 \times 10^{5}\,\mathrm{Pa/K^{1.35}})T^{1.35}\mathrm{e}^{(-126.91\mathrm{K})/T}, \quad \text{(B4)}$$

$$c_{13} = (8.0152 \times 10^{9}\,\mathrm{Pa}) - (9.1968 \times 10^{6}\,\mathrm{Pa/K})T + (1138.5\,\mathrm{Pa/K^2})T^2, \quad \text{(B5)}$$

$$B_S = (1.1204 \times 10^{10}\,\mathrm{Pa}) - (1.3836 \times 10^{6}\,\mathrm{Pa/K^{1.35}})T^{1.35}\mathrm{e}^{(-10.816\mathrm{K})/T}. \quad \text{(B6)}$$

7. Appendix C: Deviation of Fits from the Measurement Data

Figure 6 displays the deviations of the measured elastic constants c_{11}, c_{33}, and c_{12} from their polynomial fits versus temperature. The elastic constant c_{44} is not shown since it is not used for calculating B_S. The elastic constant c_{13} is not shown since it is calculated from c_{11}, c_{33}, and c_{12}; its uncertainty is provided in Sec. 2. Only the data included in the fitting are displayed in these plots (see the main text).

8. References

[1]K. Röttger, A. Endriss, J. Ihringer, S. Doyle, and W. F. Kuhs, Acta Crystallogr., Sect. B: Struct. Sci. **50**, 644 (1994).
[2]P. W. Bridgman, Proc. Am. Acad. Arts Sci. **47**, 441 (1912).
[3]T. W. Richards and C. L. Speyers, J. Am. Chem. Soc. **36**, 491 (1914).
[4]A. J. Gow and T. C. Williamson, J. Geophys. Res. **77**, 6348 (1972).
[5]T. Strässle, S. Klotz, J. S. Loveday, and M. Braden, J. Phys.: Condens. Matter **17**, S3029 (2005).
[6]R. J. Angel, J. M. Jackson, H. J. Reichmann, and S. Speziale, Eur. J. Mineral. **21**, 525 (2009).
[7]A. J. Leadbetter, Proc. R. Soc. London, Ser. A **287**, 403 (1965).
[8]R. Feistel and W. Wagner, J. Marine Res. **63**, 95 (2005).
[9]R. Feistel and W. Wagner, J. Phys. Chem. Ref. Data **35**, 1021 (2006).
[10]H. M. Ledbetter, J. Phys. Chem. Ref. Data **6**, 1181 (1977).
[11]J. B. Wachtman, Jr., W. E. Tefft, D. G. Lam, Jr., and C. S. Apstein, Phys. Rev. **122**, 1754 (1961).
[12]F. Jona and P. Scherrer, Helv. Phys. Acta **25**, 33 (1952).
[13]R. Bass, D. Rossberg, and G. Ziegler, Z. Phys. **149**, 199 (1957).
[14]A. Zarembovitch and A. Kahane, C. R. Acad. Sc. Paris **258**, 2529 (1964).
[15]V. V. Bogorodskii, Sov. Phys. Acoust. **10**, 124 (1964).
[16]T. M. Proctor, J. Acoust. Soc. Am. **39**, 972 (1966).
[17]G. Dantl, Phys. Kondens. Mater. **7**, 390 (1968).
[18]G. Dantl, in *Physics of Ice*, edited by N. Riehl, B. Bullemer, and H. Engelhardt (Plenum Press, New York, 1969), pp. 223–230.
[19]P. H. Gammon, H. Kiefte, and M. J. Clouter, J. Glaciol. **25**, 159 (1980).
[20]P. H. Gammon, H. Kiefte, M. J. Clouter, and W. W. Denner, J. Glaciol. **29**, 443 (1983).
[21]R. E. Gagnon, H. Kiefte, M. J. Clouter, and E. Whalley, J. Chem. Phys. **89**, 4522 (1988).
[22]E. Grüneisen, in *Handbuch der Physik* edited by H. Geiger and K. Scheel (Springer Verlag, Berlin, 1926), Vol. 10, pp. 1–59.
[23]A. H. A. Penny, Math. Proc. Cambridge Philos. Soc. **44**, 423 (1948).
[24]D. Helmreich and B. Bullemer, Phys. Kondens. Mater. **8**, 384 (1969).
[25]H. Suga, Thermochim. Acta **300**, 117 (1997).
[26]W. Voigt, *Lehrbuch der Kristallphysik* (B. G. Teubner Verlagsgesellschaft, Stuttgart, 1966), p. 747.
[27]D. Tromans, Int. J. Res. Rev. Appl. Sci. **6**, 462 (2011).
[28]D. T. W. Buckingham, "High-resolution thermal expansion and dielectric relaxation measurements on H_2O and D_2O ice I*h*," Ph.D. thesis, Montana State University, 2017.
[29]D. T. W. Buckingham, J. J. Neumeier, Y.-K. Yu, and S. H. Masunaga, "Thermal Expansion of Single-Crystalline H_2O and D_2O Ice," Phys. Rev. Lett. (submitted).
[30]W. F. Giauque and J. W. Stout, J. Am. Chem. Soc. **58**, 1144 (1936).
[31]S. J. Smith, B. E. Lang, S. Liu, J. Boerio-Goates, and B. F. Woodfield, J. Chem. Thermodyn. **39**, 712 (2007).
[32]G. P. Johari and S. J. Jones, J. Chem. Phys. **62**, 4213 (1975).
[33]*CRC Handbook of Chemistry and Physics*, 96th ed., edited by W. M. Haynes (CRC Press, Boca Raton, FL, USA, 2015).
[34]J. R. E. Green and L. Mackinnon, J. Acoust. Soc. Am. **28**, 1292 (1956).